GEOMORPHOMETRY 2020
PERUGIA, ITALY
JUNE 22 - 26 2020

Differences between terrestrial and airborne SFM and MVS photogrammetry applied for change detection within a sinkhole in Thuringia, Germany

Markus Zehner[§], Helene Petschko, Patrick Fischer, Jason Goetz
Friedrich Schiller University Jena,
Institute of Geography,
Grietgasse 6, 07743 Jena, Germany
[§] markus.zehner@uni-jena.de

Abstract—**Structure from motion (SFM) combined with multi view stereo (MVS) reconstruction is a cost effective method to assess topographic change, to analyse long term development and to perform risk assessments. The objective of this study was the comparison of two image acquisition methods, terrestrial handheld and UAV based photography regarding the detectable changes over time and the differences between the point clouds of the 'Äbtissingrube' – a sinkhole in Thuringia, Germany. The imagery was taken yearly from 2017 to 2019 with both UAV and handheld camera. The 3D point clouds were processed within Agisoft PhotoScan Pro. Additionally the point precisions were estimated with SFM_Georef and the differences in the resulting point clouds were compared using multiscale model to model cloud comparison with precision maps (M3C2-PM) in CloudCompare. The resulting differences are 10.2 percent of detectable change between the 2019 UAV and terrestrial point cloud with a mean detectable change of 9.0 mm. Change detection from 2017 to 2019 shows 61.1 percent of detectable change and a mean detectable change of 59.6 mm within the sinkhole. The resulting coverage of the sinkhole was generally higher by the point clouds derived from UAV in comparison to the handheld camera.**

I. Introduction

Structure from motion (SFM) and multi view stereo (MVS) reconstruction, originating from computer vision algorithms by Ref. [1], are applied widely within the analysis of earth surface processes in the last years to create dense 3D point clouds of surfaces out of optical imagery [2]. Although implemented in various open source programs, Agisoft PhotoScan Pro is preferred in many scientific publications [3]. Terrestrial handheld photography is the most basic approach, at the cost of the limitation of viewing angles and position of the sensor [4]. UAVs supporting consumer grade cameras and flight stabilisation offer better options in sensor position and viewing angles. With the low cost and weight of consumer grade cameras, highly mobile survey methods are possible, including the usage of small UAVs for image acquisition [5]. SFM has already been applied at scales from large planar regions for digital elevation model creation, landslides, rivers and sinkholes to erosion measurements within the millimeter range in laboratory work [4, 6-9]. Research comparing accuracies of point clouds derived with SFM-MVS to those of TLS and LiDAR show no disadvantages, given careful GCP placement, calibration and a sufficient number of images [2, 3, 10, 11 and 12]. Less studies have compared the differences between using terrestrial or aerial imagery [13]. As a state of the art point cloud comparison method in complex topography the multiscale model to model cloud comparison (M3C2) by Ref. [14] is often applied. Assessing the spatial uncertainties within the derived point clouds resulting from the SFM-MVS algorithms and georeferencing is decisive for identifying areas of detectable change. Profound methods have been developed with UAV imagery based on the random variations within the SFM photogrammetry workflow deriving precision maps [15] or on the comparison of repeated surveys of the same surface within a short time span [16].

The objective of this study was the comparison of two image acquisition methods - terrestrial handheld and UAV based photography - regarding the detectable changes over time and the differences between the point clouds with precision maps from the same day. The comparison was based on imagery taken of the sinkhole Äbtissingrube in 2017, 2018 and 2019.

The sinkhole is located in Northern Thuringia on the Kyffhäuser Southern Margin Fault which causes low mineralized groundwater to rise and infiltrate the overlaying sedimentary rocks of the Permian, which are very good aquifers. Solution processes caused by the water are assumed to have triggered the formation of the sinkhole [17].

Markus Zehner, Helene Petschko ,Patrick Fischer, and Jason Goetz (2020)

Differences between terrestrial and airborne SFM and MVS photogrammetry applied for change detection within a sinkhole in Thuringia, Germany:

in Massimiliano Alvioli, Ivan Marchesini, Laura Melelli & Peter Guth, eds., Proceedings of the Geomorphometry 2020 Conference, doi:10.30437/GEOMORPHOMETRY2020_53.

II. METHODS

Data was recorded yearly in autumn for 2017, 2018 and 2019 with a terrestrial and an aerial approach. The UAV was maneuvered manually to record images from above and within the sinkhole. The terrestrial imagery was taken with a handheld camera from the edge of the sinkhole. Georeferencing was accomplished with ground control points (GCPs) by surveying targets laid out around the sinkhole with a GNSS (Leica Viva GS10 & GS15). Sensor characteristics and weather conditions that influence the results of the SFM are given in Table 1 and 2. Software for the analysis was Agisoft PhotoScan Pro 1.4.3, SFM_Georef 3.1 and CloudCompare 2.10 alpha.

Within PhotoScan Pro, all images were masked by hand to the extent of the sinkhole to reduce vegetation. SFM was used to create the sparse cloud, which represents prominent features within overlapping images as tie points. This was done with a key point limit of 40,000 and a tie point limit of 10,000 with masks applied to key points and adaptive camera model fitting. With the tie points, camera positions and viewing angles were reconstructed. The sparse clouds were filtered gradually to only contain points with a reprojection error, reconstruction uncertainty and projection accuracy of 0.2, 15 and 10 for UAV data and 0.2, 30 and 10 for terrestrial imagery respectively. These settings within PhotoScan Pro were used to reduce the possible tie points of the images to only high quality ones. The lowered reconstruction uncertainty in the terrestrial sparse clouds were to ensure that the sparse clouds do not show too large holes within the slopes where unobstructed ground surfaces were visible. The GCPs were marked manually within the imagery, upon which the sparse cloud was georeferenced. Then the camera alignment was optimized with the GCPs. With MVS reconstruction, all the imagery based on the prior estimated camera positions was matched in a three dimensional dense cloud with medium quality and mild depth filtering which represents the photographed structure.

Bundle adjustment was carried out with a 10,000 fold Monte-Carlo approach to generate precision maps with SFM_Georef containing precisions of each point in the sparse clouds for x, y and z axis [9, 15].

The precision maps were combined with the dense clouds within CloudCompare with a distance based spherical normal distribution interpolation. As the sparse clouds were thinner in vegetated areas, this lead to points without precision within the dense clouds. Normals were calculated using the quadric local surface model and minimum spanning tree. Comparison of the dense clouds was done with the M3C2 plugin with precision maps enabled [14]. Cylinders are created for each core point along the local normal direction to calculate the mean distance of the two clouds. By using the precision maps variable local differences in point quality are also considered [14]. Scales for the cylinders were calculated within the plugin. For each comparison the whole cloud was set as core points. Points of the resulting comparison without a value for uncertainty were ignored as these are for the most part changes due to vegetation. Then percentage of detectable change, i.e. where the level of detection was smaller than the distance of measured change, was calculated based upon the initial cloud in each comparison. Mean and median for measured change and the level of detection were calculated for the area where detected change was observed.

Obstruction by vegetation is a large challenge with optical data, as shorter wavelengths are not able to penetrate foliage and result in local loss of surface information. To minimize the impact of the survey on the study area and to not risk any further collapse, vegetation was not cleared within the sinkhole. Furthermore any disruption by accessing the sinkhole would have impacted the results. Over the survey period, large areas at the bottom of the sinkhole became overgrown with dense vegetation so that not all vegetation within the sinkhole could be masked out.

Table 1: Survey characteristics

	Date	Lighting	Vegetation	GCPs
2017	22. March	Steep incidence	Dry brown	8
2018	22. Nov.	Diffuse lighting	Green, some snow	8
2019	05. Nov.	Steep incidence	Green	10

Table 2: Used sensors and resulting point clouds

Year	Sensor	Resolution	Focal length	Image count / used	Sparse Cloud	Dense Cloud
2017	DJI FC330	4000 x 3000	4 mm	353/353	37,037	2,651,375
	Nikon D3000	3872 x 2592	18/21 mm	221/94	13,051	2,311,397
2018	DJI FC6310	5472 x 3648	9 mm	564/542	54,443	8,767,159
	Nikon D3000	3872 x 2592	18 mm	169/157	30,820	2,402,887
2019	DJI FC330	4000 x 3000	4 mm	287/278	34,612	2,673,191
	Nikon D3000	3872 x 2592	18 mm	178/177	21,929	2,707,662

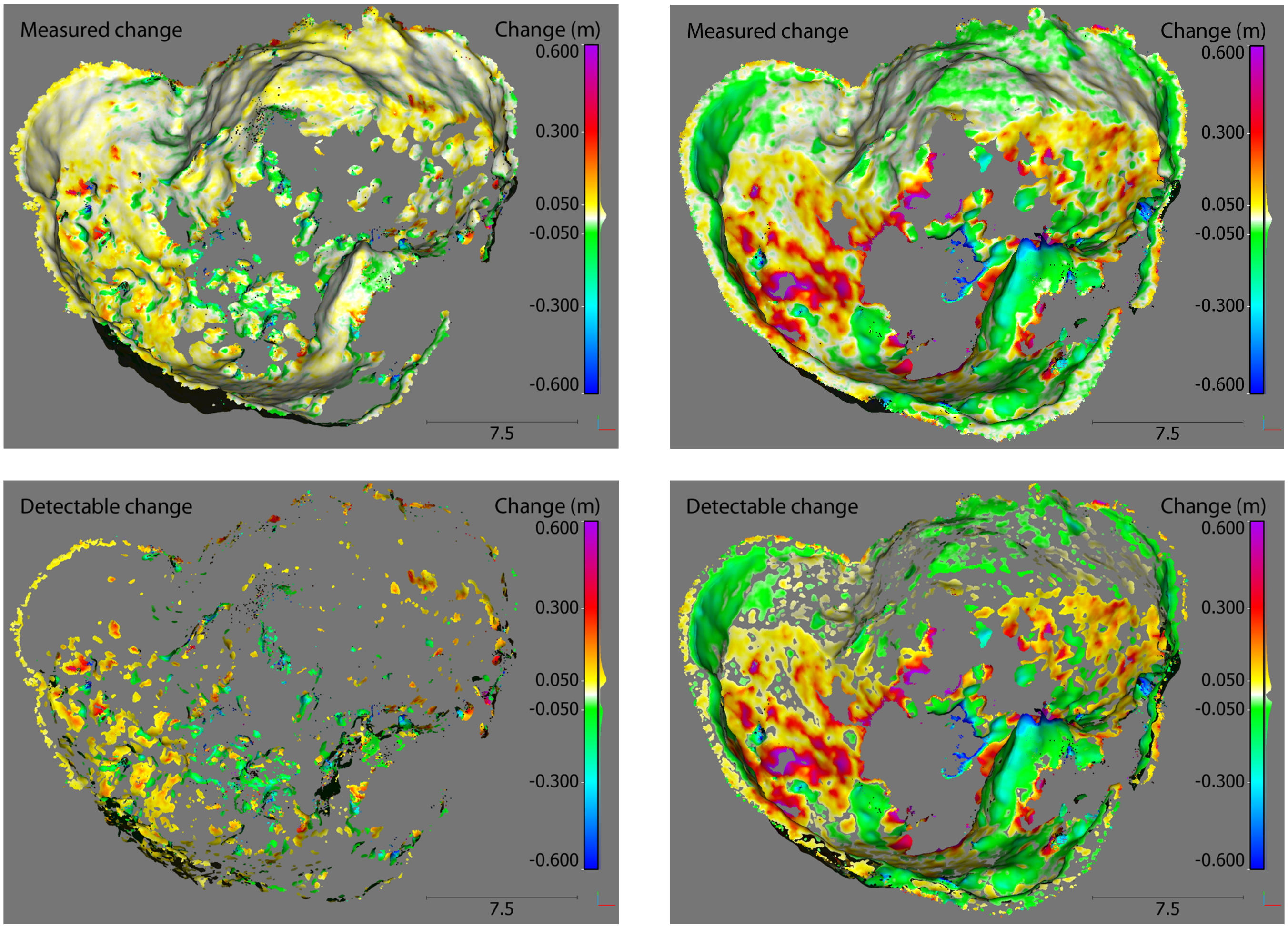

Figure 1. *Left:* Comparison of the dense clouds derived from 2019 terrestrial and aerial data, projected on the aerial cloud. *Right:* Comparison of the dense clouds derived from 2017 and 2019 aerial data, projected on the 2017 aerial cloud. Shown are points with a measured change of 0.6 m relative to the projected cloud, along with the density curve next to the color bar. The upper figures show the general measured change, where point precisions were present. The lower figures show detectable change, where the change measured was greater than the level of detection. The missing points in the figures are due to exclusion of points with measured change larger than 0.6 m, exclusion of points without point precision estimate (upper figures) and exclusion of non-detectable change (lower figures)

III. Results and Conclusions

A first result for the sensor comparison can be drawn from Table 2. The same filtering, except for a higher reconstruction uncertainty, results in more tie points out of the UAV data. The dense clouds show less difference in point count with exception of 2018. Here also the number of used images has to be accounted for: with the UAV approach, image recording was faster and more data could be acquired within each study. Manual operation of the handheld camera also lead to more blurred images, protruding branches from within the sinkhole were an additional limitation to the viewpoints. This is in line with findings from Ref. [3] as the accuracy of the point cloud does not increase linearly with the number of used images, but levels off to diminishing returns after a sufficient number [3].

The comparison of the dense clouds derived from the 2019 terrestrial and airborne data resulted in a percentage of detectable change of 10 % (273,068 out of 2,673,191, Figure 1 (on the left)). The mean and median of the measured change of the points of detectable change were 0.009 m and 0.049 m respectively with a mean and median level of detection of 0.049 m and 0.047 m. The comparison of the dense clouds derived from aerial data from 2017 to 2019 shows 61 % of points with detectable change (1,618,638 out of 2,651,375, Figure 1 (on the right)). Here the mean and median of detectable change were 0.059 m and 0.022 m with mean and median of level of detection of 0.021 and 0.018 m.

Regarding the small number of points with detectable change in the sensor comparison, we conclude that the differences between photogrammetric results are minor. Therefore, the algorithms within Agisoft PhotoScan Pro create point clouds that represent the sinkhole with comparable precision. However, the reduced viewing angles in the handheld approach lead to more obstruction in this complex relief, as well as lower visibility of the targets used as GCPs. This lead to a less complete representation of the sinkhole in the point cloud derived from the terrestrial imagery and to potentially higher errors in georeferencing. Looking at the change detection between 2017 and 2019, the survey in 2017 and 2019 had comparable lighting as well as the same sensors in use. This plays an important factor as sensor type and lighting conditions influence the precision of SFM. Deriving the precision maps and applying them within the M3C2 point cloud comparison gives us confidence in the detectable changes within the years 2017 and 2019. Over the two year period we can identify areas where material disappeared and accumulated in areas with less vegetation.

REFERENCES

[1] Ullman, S., 1979 “The interpretation of visual motion”. Proceedings of the Royal Society of London. Series B. Biological Sciences, 203(1153), 405-426.

[2] Smith, M. W., J. L. Carrivick, and D. J. Quincey. 2016. "Structure from motion photogrammetry in physical geography." Progress in Physical Geography 40.2, pp. 247-275.

[3] Eltner, A, Kaiser, A., Castillo, C., Rock, G., Neugirg, F., & Abellán, A., 2016. "Image-based surface reconstruction in geomorphometry-merits, limits and developments". Earth Surface Dynamics 4.2.

[4] Klawitter, M., Pistellato, D., Webster, A., & Esterle, J., 2017. “Application of photogrammetry for mapping of solution collapse breccia pipes on the Colorado Plateau, USA”. The Photogrammetric Record, 32(160), 443-458.

[5] Fonstad, M. A., Dietrich, J. T., Courville, B. C., Jensen, J. L., & Carbonneau, P. E., 2013. “Topographic structure from motion: a new development in photogrammetric measurement”. Earth surface processes and Landforms, 38(4), 421-430.

[6] Nakano, T., Kamiya, I., Tobita, M., Iwahashi, J., & Nakajima, H., 2014. “Landform monitoring in active volcano by UAV and SFM-MVS technique”. The International Archives of Photogrammetry, Remote Sensing and Spatial Information Sciences, 40(8), 71-75.

[7] Esposito, G., Salvini, R., Matano, F., Sacchi, M., Danzi, M., Somma, R., Troise, C., 2017. “Multitemporal monitoring of a coastal landslide through SfM-derived point cloud comparison”. The Photogrammetric Record, 32(160), 459-479.

[8] Javernick, L., Brasington, J., Caruso, B., 2014. “Modeling the topography of shallow braided rivers using Structure-from-Motion photogrammetry”. Geomorphology, 213, 166-182.

[9] James, M. R., & Robson, S., 2012. “Straightforward reconstruction of 3D surfaces and topography with a camera: Accuracy and geoscience application”. Journal of Geophysical Research: Earth Surface, 117(F3).

[10] Westoby, M. J., Brasington, J., Glasser, N. F., Hambrey, M. J., Reynolds, J. M., 2012. “‘Structure-from-Motion’photogrammetry: A low-cost, effective tool for geoscience applications”. Geomorphology, 179, 300-314.

[11] Passalacqua, P., Belmont, P., Staley, D. M., Simley, J. D., Arrowsmith, J. R., Bode, C. A., Crosby, C., DeLong, S. B., Glenn, N. F., Kelly, S. A., Lague, D., Sangireddy, H., Schaffrath, K., Tarboton, D. G., Wasklewicz, T., Wheaton, J. M., 2015. “Analyzing high resolution topography for advancing the understanding of mass and energy transfer through landscapes: A review”. Earth-Science Reviews, 148, 174-193.

[12] Cook, K. L., 2017. “An evaluation of the effectiveness of low-cost UAVs and structure from motion for geomorphic change detection”. Geomorphology, 278, 195-208.

[13] Koci, J., Jarihani, B., Leon, J. X., Sidle, R. C., Wilkinson, S. N., Bartley, R., 2017. “Assessment of UAV and ground-based structure from motion with multi-view stereo photogrammetry in a gullied savanna catchment”. ISPRS International Journal of Geo-Information, 6(11), 328.

[14] Lague, D., Brodu, N., Leroux, J., 2013. “Accurate 3D comparison of complex topography with terrestrial laser scanner: Application to the Rangitikei canyon (NZ)”. ISPRS journal of photogrammetry and remote sensing, 82, 10-26.

[15] James, M. R., Robson, S., Smith, M. W., 2017. “3-D uncertainty-based topographic change detection with structure-from-motion photogrammetry: precision maps for ground control and directly georeferenced surveys”. Earth Surface Processes and Landforms, 42(12), 1769-1788.

[16] Goetz, J., Brenning, A., Marcer, M., Bodin, X. 2018. “Modeling the precision of structure-from-motion multi-view stereo digital elevation models from repeated close-range aerial surveys”. Remote sensing of environment, 210, 208-216.

[17] Petschko, H., Goetz, J., Böttner, M., Firla, M., Schmidt, S., 2017. “Erosion processes and mass movements in sinkholes assessed by terrestrial structure from motion photogrammetry”. In Workshop on World Landslide Forum. Springer, Cham, 227-235.